Race Car Handling Optimization

Ralph Pütz · Ton Serné

Race Car Handling Optimization

Magic Numbers to Better Understand
a Race Car

Springer

Ralph Pütz
BELICON
Bayerbach, Germany

Ton Serné
SernéCM
Rosmalen, The Netherlands

Dedicated to my wife Carla and daughters Marleen, Pauline and Ellen, the most important women in my life.
Ton Serné

Dedicated to my wife Bettina, who has lovingly supported my work with advice and understanding for decades, while she always has had my back.
Ralph Pütz

Introduction

The authors of this book - both active as university lecturers and both dedicated to motorsport through their own experiences as race drivers and race engineers in various racing car racing car classes from touring cars to Formula 3 - have decided to put their theoretical knowledge of suspension technology into practical instructions for the successive development of an optimal chassis set-up.

This book is explicitly a practical course on optimising the handling of racing cars. The exploitation of the performance capacity of a racing car with regard to its handling basically means achieving maximum acceleration in longitudinal and lateral directions. Because the tyres provide the only physical contact between the mass of the car and the road, maximum acceleration is ultimately determined by the tyres. Consequently, the tyres must therefore be enabled to develop their full potential through appropriate chassis and aerodynamic settings.

This book is therefore structured as follows: First of all, it describes which basic chassis parameters are measured on the car and how. The reason for this is that most readers do not build their own racing car, but use an existing car which they must first learn to understand correctly, because without knowing the status quo, the success of changes is nothing more than pure chance.

In the further course of this book, after explaining the basics of understeer and oversteer, it is described how tyres "work" and what it takes for tyres to reach their optimum performance. All subsequent chapters serve to show how chassis geometry, suspension, shock absorbers, differentials and aerodynamics should be applied in order for the tyres to realise their potential.

The readers - amongst which hopefully also many female readers (!) - are given suggestions on the basis of numerous examples, which everyone can then apply in practice to their own vehicle.

This should help to ensure that tuning the set-up is no longer made "on instinct" but reproducibly on the basis of sound knowledge. The reward will be full seconds improvement per race lap! This is also the objective that the two authors have always had in mind, and which is the "red thread" in the book.

When explaining the theoretical relationships, basic mathematical knowledge is required, like integral calculus as well as differential equations.

Although readers with a technical university education (both at Bachelor and Masters level) can derive the most benefit from this book, an attempt has nevertheless been made to teach laypersons interested in technical and motor sport matters.

The present book in its conception as a course should indeed be read "from front to back" as the individual chapters build on each other and complement each other until they culminate in a summary.

Thanks are due to all those who have helped us writing this book, be it by provision of materials or valuable discussion.

First and foremost, the authors would like to thank Mr Werner Brückle of MoTeC Germany for his support. Thanks also go to Thomas Tahedl, Thomas Haberstock, and Johann Lehner from the University of Applied Sciences Landshut, as well as to Mr. I.J.M. Besselink and Mr. M.T.A. van der Drift from the University of Eindhoven.

We would also like to thank Mr Kees van de Grint (former tyre engineer to Michael Michael Schumacher), Daniel Pitsch, Jürgen Wohlfahrt, Danny Nowlan (ChassisSIm) and Jörge Segers for their advices. And we are grateful to the companies Bilstein and Intrax for their contributions.

Special thanks is owed to Jaz Morby and Alison Shepherd who converted the German original text into an easy-to-read English text.

Since such a comprehensive book may well contain errors even with conscientious editing, the authors are always happy to receive constructive suggestions for improvements and suggestions at any time.

Rosmalen, The Netherlands
Ton Serné BSc.

Bayerbach-Greilsberg, Germany
Prof. Dr.-Ing. Ralph Pütz

Contents

Measurement of the Setup

1

Abstract

This chapter describes how all dimensions which an engineer ought to know – like the position of the centre of gravity in three directions, wheel loads, moment of inertia, camber, caster, track, KPI, motion ratio, aerodynamic drag etc - can be measured and calculated. These dimensions will be discussed throughout the book.

The ultimate goal in racing is the continuous improvement of lap times. However, before optimisation approaches with regard to driving dynamics can be used at all, first and foremost information on the current "setup" is vital, i.e. knowing the

- weight distribution and dimensions
- current setting values of the suspension
- aerodynamic adjustment parameters.

All in all, these parameters have the essential, decisive influence on the success of lap times – over and above the tyre properties (see Chap. 3) and engine/transmission characteristics. Only through establishing this starting point – on the basis of driver feedback and/or data recording – can reliable optimisation be executed later on. The settings to be determined initially thus offer important indications of the basic tuning of the vehicle. The subsequent verification of the final, optimised setup is still done individually at the racetrack through numerous test drives (possibly with the additional support of simulation tools, see Chap. 10).

In the following, the experimental determination of all relevant vehicle-specific parameters are described, which allow an assessment of the longitudinal and lateral dynamics. (source [1]: Handbuch Rennwagentechnik)

Practice has shown that, when setup settings are changed, these are better being controlled by a second person ("four-eyes principle").

1.1 Main Dimensions and Centre of Gravity

First of all, a vehicle-specific coordinate system must be defined, to which the measured values can be related (see example in Fig. 1.1). Determining the main dimensions of a racing car including the centre of gravity are then shown as examples in Fig. 1.2. It is recommended that the measured data is always written down in tabular form, and also compared with both factory data according to the manufacturer's manual and respective regulations (see Table 1.1). The determination of both the horizontal and vertical position of the centre of gravity is described in Sects. 1.2 and 1.3.

▶   **Tip 1.1**
   The choice of the vehicle-specific coordinate system should—to avoid errors—be aligned with those coordinate systems which are applied in the data recording system used by the team and, if applicable, the vehicle dynamics simulation tool which is being used by the team.

The difference between front and rear track widths is highly significant since it can affect the self-steering behaviour of a racing car (see Chap. 5). For formula racing cars a possibly smaller rear track width can offer advantages for safety reasons, as the limited
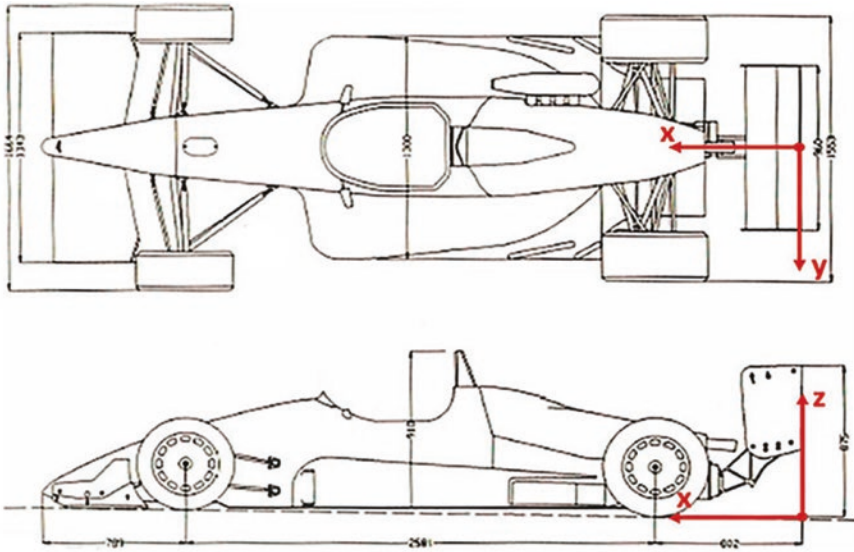
Fig. 1.1 Definition of a vehicle-specific coordinate system
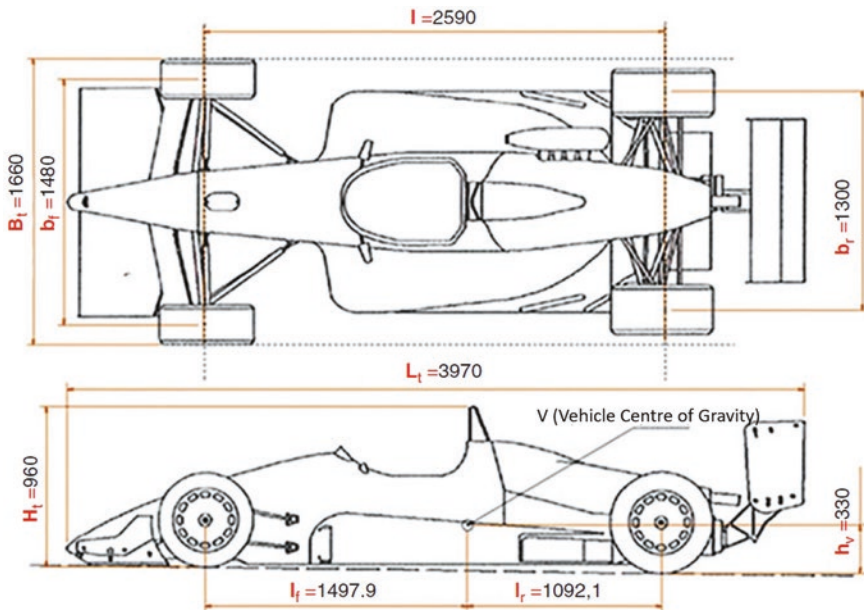
Fig. 1.2 Main dimensions of racing cars (example Reynard 903)

Table 1.1 Acquisition of the main dimensions

			Measured values	Factory specifications
Wheelbase	l	mm		
Track width front	b_f	mm		
Track width rear	b_r	mm		
Overall length	L_t	mm		
Overall width	B_t	mm		

visibility in a monoposto racing car means that the danger of the rear axle colliding side-ways when overtaking or during the starting procedure can be avoided. Also, a smaller rear track width reduces the frontal area and, hence, drag (see Chap. 8).

The dynamic track width change should be kept as small as possible, which can be achieved through optimising the chassis geometry (see Chap. 5) when cornering and bouncing both wheels on one axle. A change in track width always leads to a relative movement between tyre and road in the lateral direction (y axis), which artificially creates a slip angle and, thus, a lateral force.

This reduces the maximum lateral force that can be applied by the tyre when corner-ing (see Chap. 3), which in turn leads to lower cornering speeds and poorer lap times. In addition, due to the change in track width, straight-line driving behaviour, tyre wear and temperature increase are negatively influenced.

1.2   Static Axle Loads and Horizontal Centre of Gravity

To determine the centre of gravity distances from the front or rear axle, the static axle loads must be known. For this purpose, a weight scale under each wheel of the racing car is used to read off the corresponding value. The wheel load must be measured at an exact horizontal floor level and a correct calibration of the measuring instruments. Also, the driver must be in the vehicle and the fuel tank must be filled for half the race distance. Thus, actual race conditions can be simulated as closely as possible. From the individual wheel loads, the corresponding axle load and the total weight can be determined, see Table 1.2. Through diagonal weighing (taking the sum of front left and rear right wheel loads and the sum of the front right and rear left wheel loads), important conclusions can be reached regarding the lateral centre of gravity and, therefore, the balance of the vehi-cle (see also Sect. 6.5).

For formula racing cars, the sums determined by diagonal weighing ($m_{V,f,l}$ + $m_{V,r,r}$) and ($m_{V,f,r}$+$m_{V,r,l}$) must be identical. One exception is vehicles for oval races. Also, if an exact analysis is carried out with the driver on board and the fuel tank half full of fuel required for the full race distance, the weight proportions of the vehicle weight without driver have little effect on the percentage of the wheel loads determined (Fig. 1.3).

Table 1.2 Determining the wheel and axle loads

Wheel load front right (with driver)	$m_{V,f,r}$	Kg
Wheel load front left (with driver)	$m_{V,f,l}$	Kg
Front axle wheel load (with driver)	$m_{V,f}$	Kg
Wheel load rear right(with driver)	$m_{V,r,r}$	Kg
Wheel load rear left (with driver)	$m_{V,r,l}$	kg
Rear axle load (with driver)	$m_{V,r}$	Kg
Total mass (with driver)	$m_{V,t}$	Kg
Net weight	$m_{V,0}$	kg
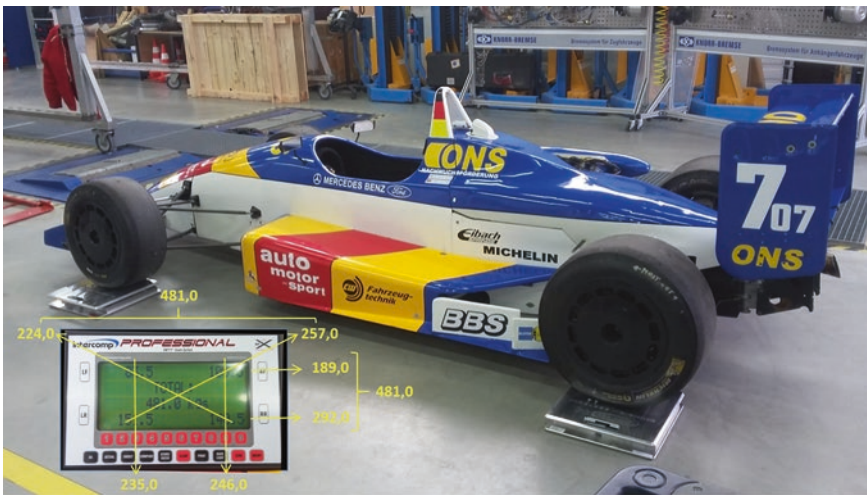
Fig. 1.3 Determining the wheel and axle loads using the example of a formula car. During the process, it was shown that both the vehicle centre of gravity and the wheel loads had significantly changed after installation of a larger battery during diagonal weighing

The measured values generally show an unequal distribution of the wheel loads from right to left. This is due to the installation position of the motor and gearbox, tank and auxiliary units such as coolers, battery, fire extinguishers etc., which can have a negative impact on the cornering behaviour of the vehicle. Corresponding approaches to solutions are discussed and described in more detail in Chaps. 5 and 8.

From the addition of the axle loads at the front $m_{V,f}$ and rear $m_{V,r}$ of the total mass m_V with the acceleration due to gravity ($g = 9.81$ m/s^2), the corresponding static normal forces follow at the front axle $F_{Z,V,f}$ and rear axle $F_{Z,V,r}$ and the weight force $F_{Z,V,t}$. Finally, establishing the balance of movements around the front axle provides the distance of the centre of gravity from the front axle l_f and from the rear axle l_r (see Fig. 1.4 and Table 1.3):
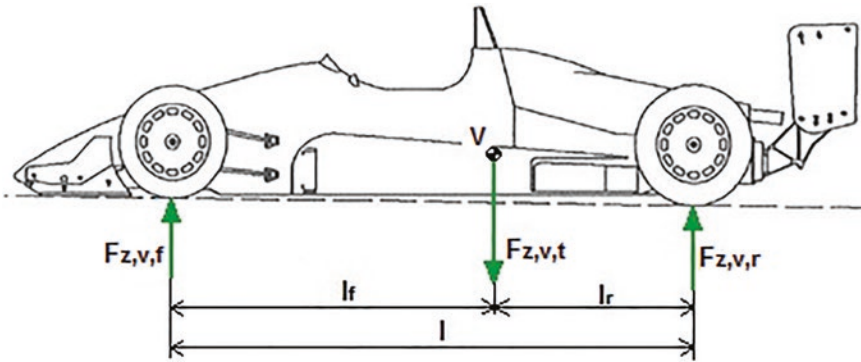
Fig. 1.4 Static axle loads (normal forces) and horizontal centre of gravity distances

Table 1.3 Determining the static axle loads and horizontal centre of gravity distances

Front to rear axle load ratio	i_m	%
Percentage of front axle load (with driver)	$Perc_f$	%
Percentage of rear axle load (with driver)	$Perc_r$	%
Centre of gravity distance from front axle	l_f	mm
Centre of gravity distance from rear axle	l_r	mm
Normal force front axle (with driver)	$F_{Z,V,f}$	N
Normal force rear axle (with driver)	$F_{Z,V,r}$	N
Weight force (with driver)	$F_{Z,V,t}$	N

$$\sum M = F_{Z,V,r} \cdot l - F_{Z,V,t} \cdot l_f = 0 \tag{1.1}$$

Solving the formula according to l_f results in

$$l_f = \frac{F_{Z,V,r} \cdot l}{F_{Z,V,t}} \tag{1.2}$$

$$l_r = l - l_f \tag{1.3}$$

with:

$F_{Z,V,r}$ Rear axle load (normal force) incl. driver and fuel tank half full for race distance, [N].

$F_{Z,V,t}$ Total vehicle weight incl. driver and tank half full for race distance, [N].

l_f Distance of front axle from the vehicle centre of gravity, [mm].

l_r Distance of rear axle from the vehicle centre of gravity, [mm].

l Wheelbase, [mm].

Fig. 1.5 Influence of the centre of gravity position on lap time using the example of the short racetrack of Le Mans (the centre of gravity of a Formula 3 car is shown)
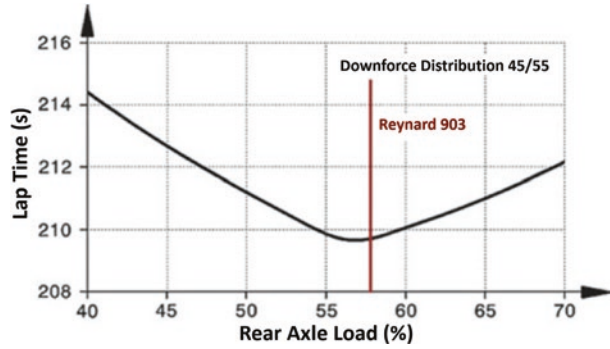
In addition, the axle load ratio and the percentage axle load shares $Perc_f$ at the front and $Perc_r$ at the rear can be determined from the normal axle forces:

$$i_m = 100\% \cdot \frac{F_{Z,V,f}}{F_{Z,V,r}} \cdot i_m \tag{1.4}$$

$$Perc_f = 100\% \cdot \frac{F_{Z,V,f}}{F_{Z,V,t}} \tag{1.5}$$

$$Perc_r = 100\% \cdot \frac{F_{Z,V,r}}{F_{Z,V,t}} \tag{1.6}$$

with:

i_m percentage front /rear axle load ratio, [%]
$Perc_f$ Front axle load percentage, [%]
$Perc_r$ Rear axle load percentage, [%]

Analysis of common racing cars with rear-wheel drive usually results in an axle load distribution of around 45% to 55% from front to rear axle. With current Formula One vehicles, the axle load distribution is approximately 40% to 60% from front to rear axle, which is due to the high torque on the rear axle. Consequently, the weight distribution is shifted in the direction of the rear axle, which leads to a basic tendency of the vehicle to oversteer as well as to greater traction when accelerating. This tendency to oversteer can be counteracted by adequate measures on the front axle, e.g. by moderate toe-in ("open setting") which offer the driver 'neutral behaviour' of the vehicle. To achieve optimum balance and fast lap times, compromises must therefore always be made and coordination under system-related consideration of all parameters must be done. This requires a comprehensive understanding of the complex relationships and dependencies which will be given in this book.

A simulation using the Le Mans racetrack as an example shows the influence of the horizontal centre of gravity position on the achievable lap time (see Fig. 1.5). Although the diagram is not valid for every vehicle and every racetrack, it provides a good point of reference for assessing the impact of the static axle load distribution of a racing car. As a result, the fastest lap times at Le Mans occur with a rear axle proportion of $Perc_r$ of 57%.

A change in the horizontal axle load distribution would be achieved by shifting the driver's seat, additional ballast weights (if the minimum weight is not reached according to regulations) or even more sophisticated solutions can be implemented, such as a system for sliding the fire extinguisher that can be operated from the driver's seat.

1.3   Vertical Centre of Gravity

In principle, the height of the centre of gravity of a racing car should be as low as possible in order to compensate for the dynamic axle load shifts both when cornering (lateral dynamics) as well as during braking or acceleration (longitudinal dynamics). The effect on brake force distribution should also not be neglected. Due to the degressive tyre characteristic curve (see Sect. 3.1), high wheel load differences when cornering will result in a loss of lateral force and, therefore, less grip. A low centre of gravity can thus reduce swaying around the longitudinal axis (x-axis) and pitching around the transverse axis (y-axis). This in turn benefits aerodynamic efficiency (see Chap. 8).

The height of the centre of gravity of a vehicle can be measured by lifting an axle, i.e. the front axle, and measuring the resulting axle load change determined (see Fig. 1.6 and Table 1.4). For this wheel load scales are placed under the rear wheels and the front axle is raised as high as possible. In order to be able to ensure sufficient ground clearance at the rear, the diffuser may have to be removed, or the lower wheels placed on a low elevation. It is recommended that the wheel suspension is blocked since the non-elevated wheels are subjected to heavier loads which could result in inaccuracies.

The centre of gravity height can be calculated using the following formula:

$$h_V = \frac{d_f}{2} + \frac{F_{Z,V,r,r} - F_{Z,V,r}}{F_{Z,V,tot}} \cdot \frac{l^2}{H_a} \cdot \sqrt{1 - \left(\frac{H_a}{l}\right)^2} \tag{1.7}$$
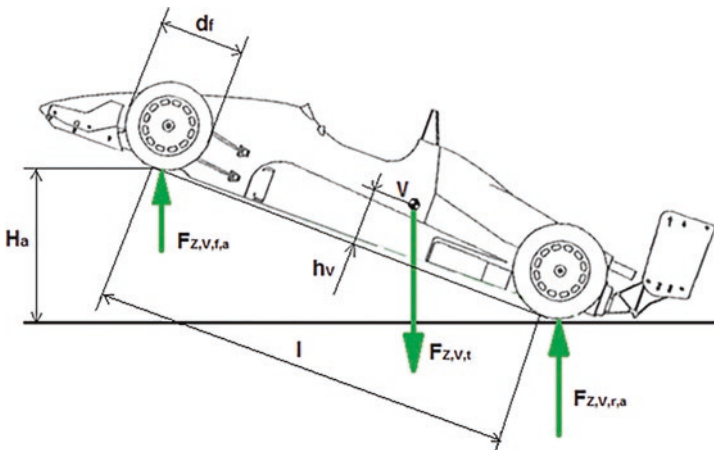
Fig. 1.6 Determining the centre of gravity height

Table 1.4 Determining the centre of gravity height	Wheel load rear right (with driver), raised	$m_{Z,V,r,r,r}$	Kg
	Wheel load rear left (with driver), raised	$m_{Z,V,r,l,r}$	Kg
	Rear axle load (with driver), raised	$m_{Z,V,r,r}$	Kg
	Height under front wheel, raised	H_a	mm
	Normal force rear axle (with driver)	$F_{Z,V,r}$	N
	Normal force rear axle, raised (with driver)	$F_{Z,V,r,r}$	N
	Weight force (with driver)	$F_{Z,V,tot}$	N
	Front wheel diameter	d_f	mm
	Normal force front axle	$F_{Z,V,f}$	N
	Wheelbase	l	mm

with:

h_V Vertical centre of gravity height, [mm]

d_f Front wheel diameter, [mm]

$F_{Z,V,r,r}$ rear axle load (normal force) incl. driver and fuel tank full for half the race distance in raised state, [N].

$F_{Z,V,r}$ rear axle load (normal force) incl. driver and tank full for half the race distance in the plain, [N]

$F_{Z,V,tot}$ total weight of the vehicle incl. driver and tank full for half race distance, N

l Wheelbase, [mm]

H_a Elevation height, [mm]

Formula 1.7 is only valid in relation to a raised front axle, with the scales measuring from the lower rear wheels.

▶ **Tip 1.2**

When determining the vertical centre of gravity, numerous measurement errors can occur.

Ensure that when lifting, e.g. with a pit jack on the chassis, that the contact surface between the jack and the vehicle is as small as possible (line contact) in order not to influence the values of the axle load change through friction on the contact surface.

Also, an exact determination of the vertical lifting height is indispensable, whereby the height of the wheel load scales of the rear axle must also be taken into account.

Furthermore, it is possible that the scales under the rear wheels will measure loads that are too low due to the fact that they are also experiencing vertical friction forces within the scales themselves.

To determine the centre of gravity height, it is advisable that only high-quality wheel load scales are used.

1.4   Moment of Inertia at Vertical Axis

The mass moment of inertia is the resistance of a body against change of its position around a certain axis, in this case the vertical axis of the vehicle (z-axis). In order to implement a quick change of position, all heavy masses should be arranged near the centre of gravity. In the case of a racing car, lower mass moment of inertia around the vertical axis leads to more agile driving behaviour, i.e. a faster reaction to steering movements.

To calculate the mass moment of inertia around the vertical axis, the following approximation, derived in numerous practical tests for vehicles in the range of 650–1500 kg up to a total length L_t of 6 m, can be applied with an accuracy of 97%:

$$J_z = 0.1269 \cdot m_{Z,V,tot} \cdot l \cdot L_t \tag{1.8}$$

with:

J_z Moment of inertia around the vehicle vertical axis, [kg m^2]
$m_{Z,V,tot}$ Total vehicle mass incl. driver and fuel tank filled for half the race distance [kg]
l Wheelbase, [mm]
L_t overall length, [mm]

The mass moment of inertia J_z around the vertical axis can be determined approximately by experimenting with manageable expenditure. A simple torsional oscillation system can be built (see Fig. 1.7 left). Here the oscillating effect is created by a thread
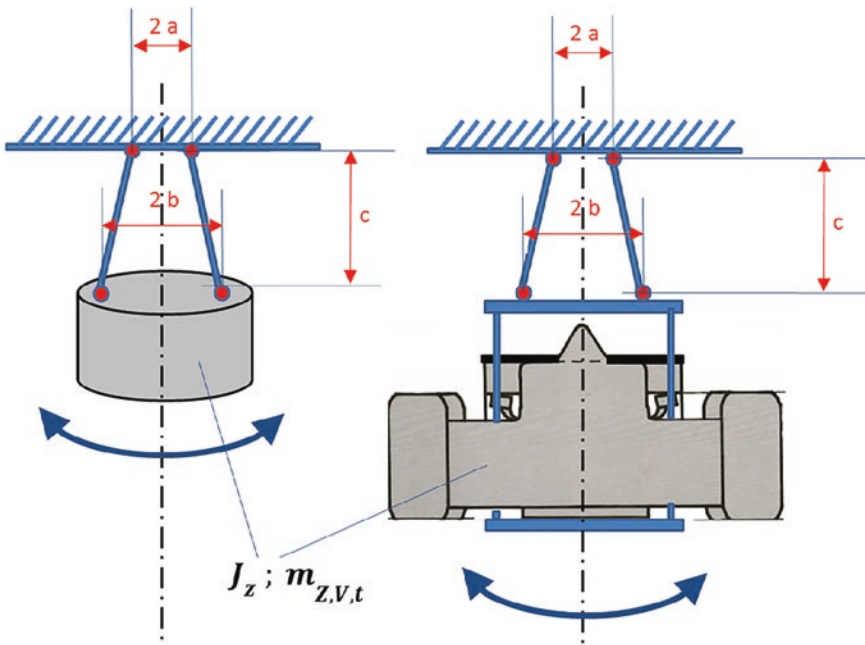
Fig. 1.7 Determining the moment of inertia with multi-thread suspension

suspension (on professional test stands via a torsion bar suspension with defined torsional stiffness). The damping of the oscillator can be disregarded.

The vehicle mass $m_{Z,V,tot}$ is measured by turning the thread suspension around the vertical vehicle axis (z-axis) by up to 45° and the duration period T_0 of several oscillations is determined. The position of the vertical axis is determined by the horizontal position of the vehicle's known centre of gravity. Iterations are carried out to improve accuracy.

If necessary, relative error can be determined in percent by an error calculation.

Due to non-linear equations of motion, small skew angles of the threads in the deflection are recommended. Long threads (c >>; c>>re advantageous for this.

Usually the thread suspension is attached to the ceiling of the workshop. The design of the suspension device should be such that its mass moment of inertia J_{AV} is negligible. An exemplary suspension device is shown in Fig. 1.8.

With the geometrical dimensions of the yarn suspension (a, b, c) and the measured.

period T_0 of oscillation, the mass moment of inertia of the racing car around the vertical axis (with negligible mass moment of inertia of the suspension device) results in:

$$J_z = \frac{m_{Z,V,tot} \cdot g}{4\pi^2} \cdot T_0^2 \cdot \frac{a \cdot b}{c} \tag{1.9}$$
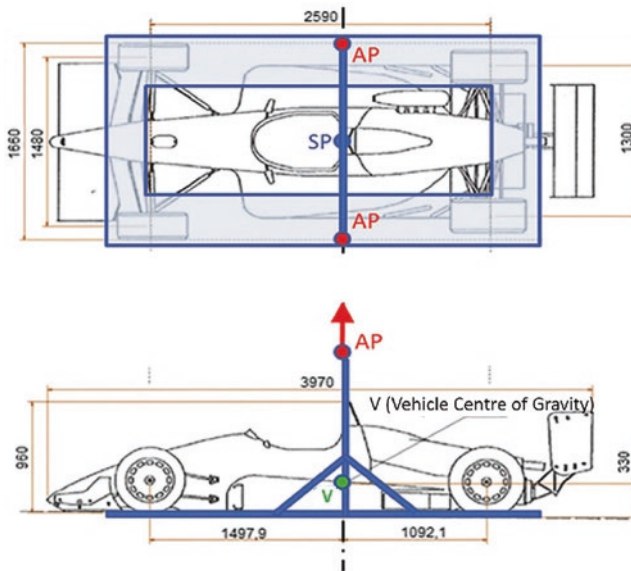
Fig. 1.8 Example of a simple suspension device with multi-thread suspension

where:

J_z	mass moment of inertia of the racing car around the vertical axis, [kg m^2].
$m_{Z,V,tot}$	total vehicle mass incl. driver and fuel for half the race distance. (also including negligible suspension device), [kg]
T_0	measured period duration of the torsional oscillation around the z-axis, [s]
a, b, c	Dimensions according to Fig. 1.7, [m]
g	Acceleration due to gravity, [m/s^2]

It is recommended that, if possible, a large length c should be chosen to improve accuracy of the experiment. A mathematically experienced race car engineer uses the mass moment of inertia around the vertical axis also for simulation calculations of the rotation of the vehicle around the vertical axis (yaw), e.g. on the basis of a single-track vehicle model, which provides basic statements on lateral dynamics (see Chap. 2, Fig. 2.5).

The mass moments of inertia around the longitudinal axis (x-axis) and transverse axis (y-axis) can also be determined using a similar test setup as shown in Figs. 1.7 and 1.8. Thus, it is apparent that the frequencies of the (natural) oscillations around the respective axes are not identical.

Example 1.1

A monoposto with driver weighs only 536 kg. The wheelbase is 2.59 m and the total length 3.97 m. Although it can be calculated using the formula 1.8 (which normally only starts at 650 kg), with the result that there are minor deviations from the actual moment of inertia, this approach nevertheless serves as a very good approximation method. With the corresponding values, the mass moment of inertia to be calculated is:

$$J_z = 0.1269 \cdot 536\,\text{kg} \cdot 2{,}59\,\text{m} \cdot 3{,}97\,\text{m} = 699.4\,\text{kgm}^2$$

The same monoposto is now used for a torsional oscillation test around the vertical axis (z-axis) according to Fig. 1.7. The yarn suspension clamped on the ceiling is $2 \cdot a = 1$ m; on the vehicle $2 \cdot b = 1.6$ m. The vertical projection of the thread length (clamping height) is $c = 3.0$ m. Over five tests á 10 oscillations the measured period duration is 6.2 s. With these values the mass moment of inertia is:

$$J_z = \frac{536 \cdot 9.81}{4\pi^2} \cdot 6.2^2 \cdot \frac{0.5 \cdot 0{,}8}{3} = 682.6\,\text{kgm}^2$$

The difference in this case is less than 3%! ◄

▶   **Tip 1.3**

A low mass moment of inertia is the result of various constructive measures. In addition to a mid-engine concept as the optimum, the arrangement of the fuel tank in formula racing cars directly behind the driver and the placement

of the radiators and the battery/electronics in the side pods lead to a mass concentration close to the CoG.

   With touring cars there is often a difference in the distribution of mass between right and left. However, this can be advantageous, e.g. if the centre of gravity is more to the right on racetracks driven clockwise, due to a smaller difference in the normal forces between the inner and outer tyres of the curve (see Chap. 5). Most racetracks are driven clockwise and show more right turns.

1.5   Suspension Measurement

In relation to the driving dynamics of a race car, the chassis settings:

- camber
- track
- and
- Kingpin inclination (KPI).

(besides the centre of gravity position and the resulting axle load) are decisive. Therefore, it is recommended that these values are determined using modern laser measurement technology. In the following these parameters and their effects on driving behaviour are investigated. In Chap. 5 (geometry), the effects of these settings are analysed in more detail.

1.5.1   Camber

A widespread way of influencing driving behaviour in motor racing is the adjustment of the vehicle-specific camber ε (static camber). This is the inclination of the wheel in lateral direction (y-axis) to a vertical through the wheel contact point (see Figs. 1.9 and 1.10). A distinction is made between positive and negative camber. A wheel tilted outwards at the top shows a positive camber and a wheel tilted inwardly shows a negative camber angle. However, the decisive factor is the so-called road-specific camber (absolute camber, see also Chap. 5). If a wheel is inclined at the top towards the centre of the curve, it is defined as a negative road-specific camber. The aim must be to achieve a negative road specific camber on all four wheels (vehicle specific: inner wheels positive camber, outer wheels negative camber). In this way, at a constant slip angle, higher lateral forces can be transferred (also see Fig. 3.1).

   It is recommended that the measured values be compared with the factory specifications (see Table 1.5).

   As a rule, the measured values for racing cars show negative vehicle-specific camber values on both the front and rear axles. Due to the negative camber, the deformation of
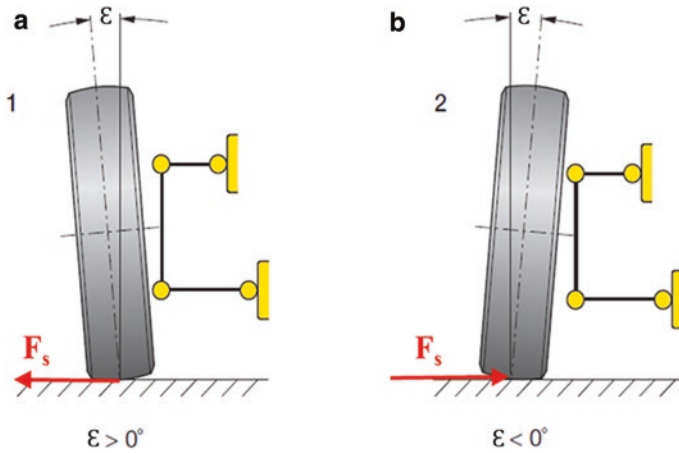
Fig. 1.9 Positive camber **a** and negative camber **b**

Fig. 1.10 Example depicting the determination of the camber on the front axle with modern laser measurement technology. The steering wheel should be positioned 'straight ahead'; the value can be read directly on the camber gauge, which is set on the axis of the measuring head

Table 1.5 Determination of the camber values on the front and rear axle

	Measured values	Factory settings
Camber front right $\varepsilon_{f,r}$		
Camber front left $\varepsilon_{f,l}$		
Camber rear right $\varepsilon_{r,r}$		
Camber left rear $\varepsilon_{r,l}$		

the tyre sidewall when cornering is reduced, resulting in an even greater load on the tyre contact patch (see also Figs. 3.17 and 3.18). Consequently, higher lateral forces can be transmitted.

Even if the wheel travels of a race car are extremely low, especially a monoposto, with travels of between 25 and 40 mm, the effects on the wheel position – viewed

superficially—are minimal, the consequences of this change in wheel position for driving behaviour must not be disregarded.

Movement of the car body during cornering around the longitudinal axis (x-axis: roll) can lead to a change in the camber angle of individual wheels (see Chap. 5). This also has an effect on the performance of the of the tyre, because negative camber reduces the spring stiffness of the tyre C_T (see Chap. 3). Basically, the road-specific camber angle of a wheel should be kept as constant as possible along its wheel travel.

1.5.2   Track

A distinction is made between toe-in and toe-out. If a wheel viewed from above in the direction of travel points towards the centre of the vehicle, it is referred to as toe-in, and if the wheel points towards the outside, it is referred to as toe-out (see Fig. 1.11). With a toe-in position a lateral inward force is imposed on both tyres and thus a stable straight line is ensured. Without the toe-in, the tyre would not be able to build up any pre-tension, which is then translated into a lateral force (see Chap. 3). When measuring the toe, it is imperative that the front axle is positioned exactly straight.

For this, a three-step procedure is recommended (see Fig. 1.12 and Table 1.6):

- First adjust both track rods to exactly the same length.
- Centre and fix the steering rack.
- For all changes in direction of toe-in or toe-out, turn the steering rack of both track rods by equal amounts.

In principle, any change in toe should be avoided with vertical wheel movements, because the nose of the vehicle no longer follows the line specified by the driver. This undesired steering movement of the wheels is known as "Bump Steering". If, for example, a car brakes for a corner, the outer wheel is in bump and remains in bump during
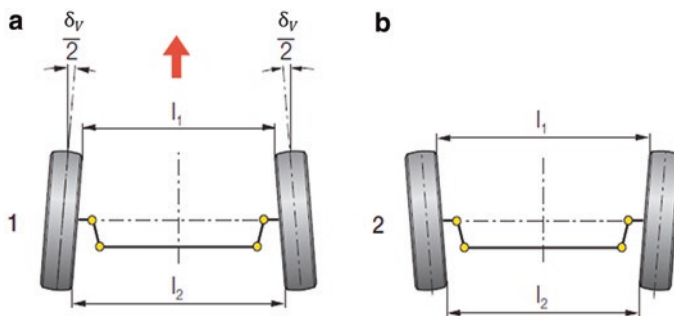
Fig. 1.11   **a** toe-in ($l_1 < l_2$; $\delta_V > 0$) and **b** toe-out ($l_1 > l_2$; $\delta_V < 0$)

Fig. 1.12 Example of an alignment device for the determination of the track (e.g. toe-out) on the front axle with modern laser measuring technology. First, the alignment device must be placed in front of the front axle and adjusted in such a way that the lasers of both sides point to "zero"; then the alignment device is set at a defined distance (e.g. 3.40 m) to the rear as shown in this figure. After shifting the alignment device to "zero" for one side, the toe value can be read off the scale on the other side

Table 1.6 Determination of the toe angle on front and rear axle

	Measured values	Factory settings
Front toe angle $\delta_{V,f}$		
Toe angle rear $\delta_{V,r}$		

turn in (Phases 1 and 2, see Sect. 2.3.1) Due to the heavy load on this outer wheel, this wheel—to a large extent—dictates the direction of the car movement. However, the inner wheel moves from bump into rebound, hence it undergoes a large wheel travel. If the geometry of the steering mechanism causes bump steer, this inner wheel will result in a marked toe-change, which destabilizes the front of the car. In this case, a problem with the shock absorbers is often thought to be the cause, whereas the actual reason is the geometry of the steering mechanism. Measures to prevent "bump steering" are described in Chap. 5.

▶   **Tip 1.4**

For a front-wheel driven racing car, with rubber suspension pivots, a static toe-out is often set, such that the traction forces will push the suspension forward, resulting in a dynamic neutral toe or even toe-in (depending on the lay out of the suspension).

A static toe-out says nothing about the actual, dynamic track setting. If the pivoting points are now changed to uniballs, the original setting of a static toe-out would no longer be sensible.

1.5.3   Caster

The caster angle is the angle between the steering axis and a vertical through the centre of the wheel in side view (see Fig. 1.13 and Table 1.7). With a double wishbone suspension of formula cars or prototypes, the steering axis is often the virtual connection between upper ball bearing and lower supporting joint (see. Fig. 1.14).
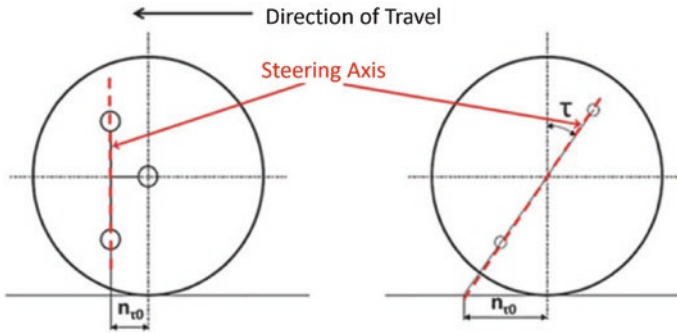
Fig. 1.13   Caster angle τ and caster trail $n_{\tau 0}$

Table 1.7   Determination of the caster angle on the front axle (steering axle)

	Measured values	Factory settings
Caster angle front right $\tau_{f,r}$		
Caster angle front left $\tau_{f,l}$		

Fig. 1.14   Example of the steering axis of a double wishbone suspension with the KPI angle σ
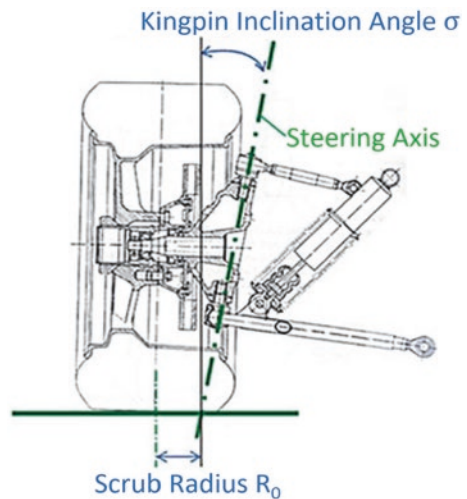
One task of the caster is to ensure stable straight-line travel, comparable with a wheel of a supermarket trolley. A positive caster angle means that the point of intersection of the steering axis through the road surface is located in front of vertical through the wheel centre.

This creates a lever arm which, besides the KPI, scrub radius R_0 (see Sect. 1.5.4) and the caster trail, is responsible for a 'self-steering' power from the tyre. This self-steering power caused by KPI and caster is not to be confused with the 'self aligning torque' seen in the tyre's contact patch.

Usual values for the caster angle of racing cars are between $+2.5°$ and $+4.5°$. For touring cars, caster angles up to $+8°$ and even greater are used.

In the 1980s, the age of the so-called wing cars, sometimes even negative caster angles were common, i.e. the point of intersection of the steering axle was behind the wheel centre point. Due to the very high downforce, caused by the "ground effect", the small steering wheel diameters can result in extreme steering forces for the driver. Due to the negative caster trail, the centrifugal forces help the front wheels turning inwards.

Another reason why cars have a positive caster, is to influence change on the camber angle when steering. Due to the KPI and caster angles, the steering axle is not perpendicular to the road, but inclined. This inclination causes the wheel to move around an inclined axle when steering, which means that the inner wheel has a positive and the outer wheel a negative camber change. The changes must be added to the static vehicle-specific camber to obtain the total dynamic camber (also see Fig. 5.3). As a result, higher lateral forces can be transferred and, thus, higher cornering speeds can be achieved (see Chap. 5).

In contrast, the caster for front-wheel driven cars τ can also be close to 0°.

1.5.4   Kingpin Inclination (KPI) and Scrub Radius

The kingpin inclination angle σ is the angle between the steering pivot axis and a

vertical to the ground, arranged parallel to the vertical axis of the vehicle (Fig. 1.14) with the wheel at $0°$ camber. Compared to the caster angle, this time the steering axle is positioned in the transverse plane of the vehicle examined. The so-called scrub radius or steering roll radius (Fig. 1.15) is the distance between the wheel contact point and the point of intersection of the extended steering pivot axis through the road as a projection on a plane perpendicular to the direction of travel.

Due to the KPI, the wheel also describes a curve when steering, which slightly raises the vehicle body on the front inner wheel and slightly drops the body on the front outer wheel. This is called 'roll-steer' and it causes the load on the inner wheel to be increased. Through the inclination from KPI and caster the wheel is pushed back in a straight, forward position by the vehicle mass, resulting in a self-aligning behaviour of the car. A disadvantageous property of the KPI is the resulting road-specific camber change in the positive direction. This is, however, less than the camber change due to caster. The
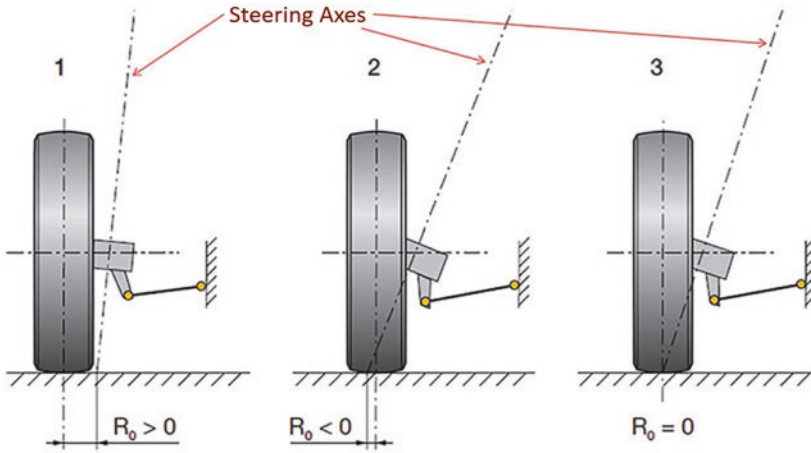
Fig. 1.15   Steering roll radius R_0 as a function of the steering axle position

Table 1.8   Determination of KPI and Scrub Radius

King Pin Inclination σ		o
Scrub Radius R_0		mm

adapted design of the geometry of the suspension (see Chap. 5) means that this effect can be reduced or even eliminated. The values for the angle of KPI in today's racing cars are usually between 5° and 8° (see Table 1.8).

1.5.5   Steering Angle and Toe Angle Difference

The static angle difference between the steered front wheels (also known as the Ackermann angle $\Delta\delta_A$) is the angle between the inside and outside wheels when the steering is applied.

This static value is valid only for extremely slow, quasi-stationary cornering (Ackermann condition). Due to the smaller corner radius on the inner wheel, there is a larger kinematic steering angle δ_i required than on the outer wheel $\delta_{A,o}$, see Fig. 1.16. Dynamically both wheels move into toe-out relative to one another.

The measurement of the toe difference angle is carried out at steering angles to the left and right to detect any deviation.

If there is no difference in the steering angle between the two front wheels, a higher wear and tear of the tyres occurs when cornering. Optimum tyre temperatures will not be achieved. The steering geometry is usually designed in such a way that, with an increasing steering angle, the toe difference angle changes too, taking the dynamic tyre slip angles into consideration.
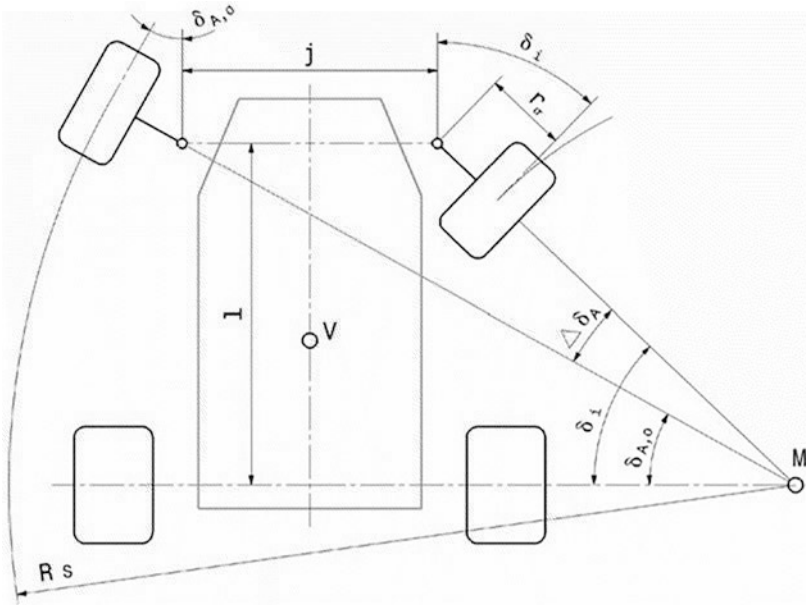
Fig. 1.16 Kinematic relationships during static cornering with pure rolling around the corner centre M (Ackermann condition). The difference between the steering angle on the outer wheel $\delta_{A,o}$ and the steering angle on the inner wheel δ_i is the toe difference angle $\Delta\delta A$ (Ackermann angle) where: l wheelbase, V centre of gravity of the vehicle.

Determination of the static toe difference angle is vital to detect any incorrect setting of the steering mechanism.

It should be noted at this point that at higher speeds, due to the steering forces during cornering, the slip angles in the tyres increase, which cause the kinematic steering angles to differ from the actual dynamic steering angles (see Fig. 5.18).

Example 1.2

Following a collision on the right front wheel during a race, the toe change of a Formula racing car is measured which reveals that the steering kinematics have been adjusted or even damaged (see Fig. 1.17). A check of all the steering systems elements is required for safety reasons. ◄

In the case of double wishbone axles, camber is often adjusted by turning the upper ball joints on the upright, which leads to a change in length of the upper wishbones.

In this context, it should be noted—especially with regard to Chap. 5—that it is highly recommended that the geometries of the suspension control arms and their